



Research paper

## Planktonic foraminifera in the sediment of a western boundary upwelling system off Cabo Frio, Brazil



Douglas Villela de Oliveira Lessa<sup>a</sup>, Rodrigo Portilho Ramos<sup>a</sup>, Catia Fernandes Barbosa<sup>a</sup>, Aline Roberti da Silva<sup>a</sup>, Andre Belem<sup>a</sup>, Bruno Turcq<sup>b</sup>, Ana Luiza Albuquerque<sup>a,\*</sup>

<sup>a</sup> Departamento de Geoquímica Ambiental, Universidade Federal Fluminense, Niterói, Rio de Janeiro, Brazil

<sup>b</sup> LOCEAN – Paleoproxus, Institut de Recherche pour le Développement, Bondy, France

### ARTICLE INFO

#### Article history:

Received 22 January 2013

Received in revised form 25 November 2013

Accepted 28 December 2013

#### Keywords:

Southwest Atlantic  
Foraminiferal assemblage  
Similarity percentage  
Upwelling  
Holocene

### ABSTRACT

The distribution of planktonic foraminifera in box-core tops under the influence of a western boundary upwelling system along the southeastern Brazilian continental margin was examined to evaluate the similarity percentage (SIMPER) and to create a biofacies model for paleoenvironmental applications. Species associated with warm and oligotrophic water were distributed in the Rio de Janeiro sector of the Campos Basin, while productive water species were most abundant in the Rio de Janeiro sector of the Santos Basin, and cold-water species were most abundant in the Cabo Frio Upwelling System (CFUS). Four major biofacies are associated with the oceanographic setting of the CFUS: one from the Campos Basin (A – Brazil Current front), one from the Santos Basin (B – mixture of coastal and oceanic waters), and two associated with the Cabo Frio High in the northern biofacies (C) and southern biofacies (D). The distribution of biofacies C and D was associated with temperature differences. Biofacies C represents a mixture of upwelling and tropical waters, while biofacies D represents a mixture of cold, nutrient-rich and Santos Basin waters. These biofacies were also defined in core CF10-01B, in which six main paleoceanographic phases were characterized during the last 9 cal kyr, predominantly showing alternating dominance between biofacies C and D. From 9.0 to 5.0 cal kyr before the present (BP), the system was dominated by biofacies C. Between 4.0 and 3.5 cal kyr BP, biofacies D was dominant. Between 3.5 and 2.5 cal kyr BP, a strong influence of coastal waters and weakened upwelling activity were indicated by the dominance of biofacies B + C + D. The last 2.5 cal kyr was dominated by biofacies D. The SST in this core was reconstructed using the Modern Analog Technique (MAT), which revealed 0.35 °C of variability, indicating no SST changes during the Holocene. The weak sensitivity of the MAT was due to the interplay among different oceanographic features.

© 2014 Elsevier B.V. All rights reserved.

### 1. Introduction

Planktonic foraminifera have been widely used to decipher paleoceanographic changes because their distribution is strongly influenced by temperature, salinity, upper water stratification and food availability (Bé and Tolderlund, 1971; Niebler et al., 1999) and because the CaCO<sub>3</sub> tests of these foraminifera may be well preserved in the sediment. Many studies have examined the distribution and ecology of these species based on fossil assemblages in sediments (Thunell, 1978; Hilbrecht, 1997; Martinez et al., 1998; Ding et al., 2006), sediment traps and plankton nets (Bé and Tolderlund, 1971; Bé, 1977; Boltovskoy et al., 1996; Kuroyanagi and Kawahata, 2004), and laboratory cultures (Caron et al., 1981; Bijma et al., 1990).

Changes in the communities of planktonic foraminifera are observed over short distances in confluence zones and upwelling areas (Little

et al., 1997; Kuroyanagi and Kawahata, 2004; Peeters et al., 2004; Chiessi et al., 2007; Souto et al., 2011). In this context, it is crucial to understand the regional oceanographic characteristics of the study area to determine which species best reflect the environmental conditions.

Several mathematical and statistical models, in addition to geochemical proxies, have been used to reconstruct the environmental conditions of the past. Sea surface temperature (SST) has been the environmental variable that has been most explored, through statistical calibration methods for transfer functions (Malmgren et al., 2001; Kucera et al., 2005) and through the geochemical analysis of tests, including those based on oxygen stable isotopes ( $\delta^{18}\text{O}$ ) and the Mg/Ca ratio (Anand et al., 2003; Mulitza et al., 2003).

The Modern Analog Technique (MAT, Hutson, 1980) and its variants, such as SIMMAX (the acronym representing MAT plus a similarity index, Pflaumann et al., 1996) and the revised analog method (RAM, Waelbroeck et al., 1998) are the methodologies that are most commonly used to reconstruct SST in downcore foraminiferal assemblages. These techniques compare the similarity between recent core-top planktonic foraminiferal assemblages found in an area (or globally) that are associated with an SST value and fossil assemblages in the studied core. SST

\* Corresponding author at: Departamento de Geoquímica, Universidade Federal Fluminense, Outeiro São João Batista, s/n, Centro, Niterói, Rio de Janeiro CEP 24020-150, Brazil. Tel.: +55 21 26292197; fax: +55 21 26292234.

E-mail address: [analuiza@geoq.uff.br](mailto:analuiza@geoq.uff.br) (A.L. Albuquerque).

values are typically chosen from the 10 best analogs (the most similar assemblages) to determine the reconstructed SST (Malmgren et al., 2001). However, according to Portilho-Ramos et al. (2006) and Pivel et al. (2013), SSTs reconstructed using the MAT are considered to be underestimated in certain regions, such as the Southwestern Subtropical Atlantic, where changes in the foraminiferal species that live below the thermocline (which constitutes cooler assemblages) occurred in the Early Holocene. Therefore, changes in the central-intermediary layer could lead to dissimilarity with recent databases, thus influencing the reconstructed SST.

The objectives of this study were to characterize the geographical distribution of recent planktonic foraminifera by studying surface sediments from the Rio de Janeiro continental margin (RJCM), to contribute to our knowledge of the ecological role of the most abundant species found in the RJCM, and to develop a biofacies model based on similarity

percentage (SIMPER) analysis for application in paleoceanographic studies. The model developed in this study was associated with core-top modern analog assemblages, similar to the MAT. We used this model to reconstruct the effects of different oceanographic conditions within the studied area using similarity values. Three types of water masses influence the region analyzed in this study: Coastal Water, Tropical Water and South Atlantic Central Water (SACW). These water masses were determined based on the species compositions of the assemblages, permitting the inclusion of thermocline layer species and, thus, reducing the paleoceanographic reconstruction bias.

## 2. Oceanographic setting

The Santos and Campos Basins are located in the RJCM. The boundary between these basins is represented by the Cabo Frio High, and the Cabo

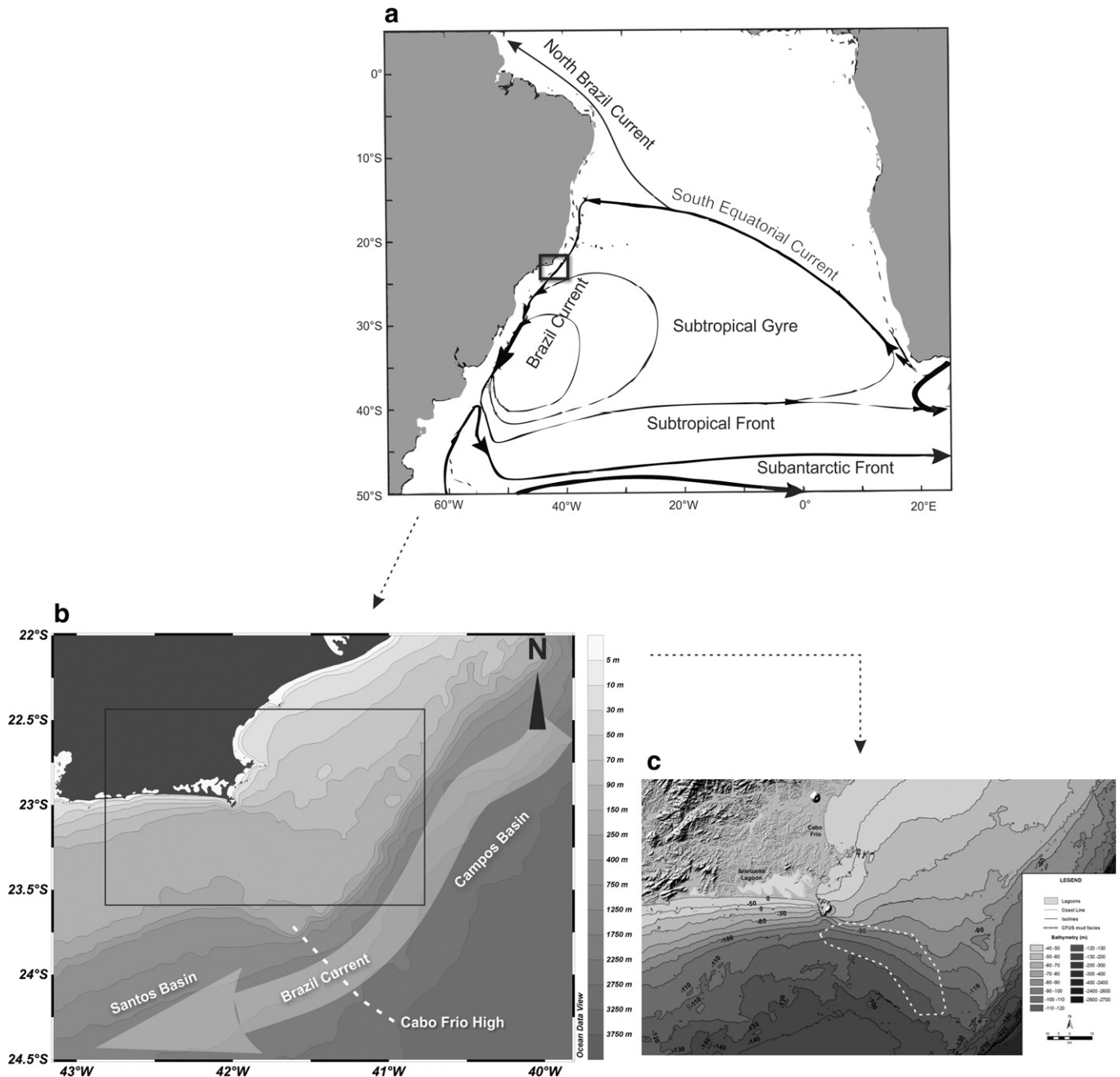


Fig. 1. (a) Oceanographic characterization of the Subtropical Atlantic (modified from Stramma and England, 1999), (b) the bathymetry and topography of the RJCM and (c) the continental shelf off Cabo Frio, highlighting the location of the CFUS mud facies (dashed polygon).

Frio Upwelling System (CFUS) is the most prominent oceanographic feature in the region (Fig. 1). The CFUS is characterized by a cold SST anomaly during the beginning of the austral summer (December and January, Fig. 2d) that is highly influenced by the intense NE winds from the Subtropical South Atlantic High (Valentin, 1984). During the austral winter, the NE winds are weaker and the frequency of frontal systems with SW winds is higher, favoring the influence of warm surface waters from the Brazil Current in the region (Fig. 2b).

In the CFUS, the NE trade winds impose an offshore flux of the Tropical Water, inducing upwelling of SACW on the coast of Cabo Frio and the presence of SACW in the photic zone over the middle and outer shelf. The SACW is eventually pushed offshore by tidal movements, reaching the front of the Brazil Current. The interaction between Tropical Water and the cold upwelling plume often forms surface–subsurface cold core meanders and eddies that favor the uplift of deeper water masses. Campos et al. (2000), Silveira et al. (2000), Rossi-Wongtschowski and Madureira (2006) and Calado et al. (2010) have described this phenomenon contributing to the occurrence of SACW in the photic zone of the continental shelf, which characterizes the CFUS.

Coastal Water occurs along most of the inner shelf of the RJCM. Coastal Water is influenced by river discharge, estuarine waters and shelf waters, and it is therefore characterized as a productive water mass with low salinity (<34 psu) and high temperature (>20 °C) (Rossi-Wongtschowski and Madureira, 2006). Tropical Water is present along the first 200 m of the Brazil Current and originates in equatorial latitudes. Thus, Tropical Water is oligotrophic with a high temperature (>22 °C) and salinity (>36 psu). SACW forms the sub-surface layer of the Brazil Current (flowing at a depth between 200 and 800 m) that flows along the continental shelf break. It is a productive water mass with a low temperature (between 6 and 20 °C) and medium salinity (34.5–36 psu) (Silveira et al., 2000; Rossi-Wongtschowski and Madureira, 2006).

The northern RJCM (southern Campos Basin) is generally characterized by warm oligotrophic waters because of the presence of a more stable flux of the Brazil Current (Fig. 2). Such stability occurs between the Vitória–Trindade submarine chain and the Cabo Frio High at 23°S, where the coastline and continental margin change their orientation and the flow of the Brazil Current tends to move offshore (Rossi-Wongtschowski and Madureira, 2006).

The southern RJCM (northern Santos Basin) encompasses several water masses due to the offshore flux of the Brazil Current in the CFUS. The meanders and eddies in the RJCM bring shelf waters, upwelled SACW coastal plumes and oligotrophic offshore waters towards the CFUS (Calado et al., 2006). These contributions from several sources, under a multiannual perspective, characterize the occurrence of productive waters.

### 3. Materials and methods

#### 3.1. Sampling, dating and micropaleontological analyses

Our database consisted of 34 box-core tops (Fig. 3, Table 1): fifteen box-core tops (0.5 to 1.0 cm thick) were collected within the CFUS as part to the Ressurgência (this study) and CLIMPAST (Souto et al., 2011) projects, and an additional nineteen box-core tops (2 cm thick) were collected by the Living Resources of the Brazilian Economic Exclusive Zone (REVIZEE) project on the continental shelf and upper continental slope of the Santos and Campos basins, adjacent to the CFUS.

A 382-cm-long gravity core (CF10-01B) was obtained from a water depth of 128 m in the CFUS at 23.4°S and 41.6°W. This core was used to verify the application of the biofacies defined using the surface samples in a paleoenvironmental reconstruction and to identify possible sources of error. Here, biofacies are defined according to Stemmann and Johnson (1992) as multivariate clusters of species frequencies within a

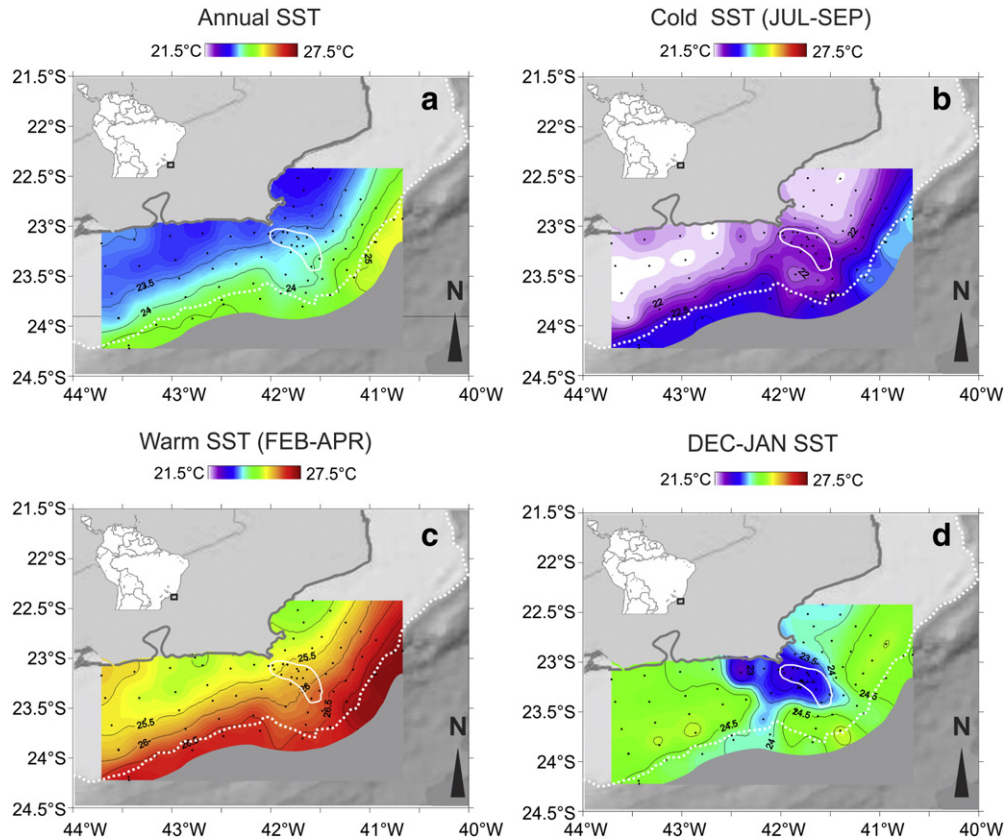


**Fig. 2.** 2002–2010 average satellite SSTs for the RJCM (black dots) extracted from (<http://las.pfeg.noaa.gov/oceanWatch/oceanwatch.php>). (a) Total average SST; (b) average warmest SST (February, March and April); (c) average coldest SST (July, August and September); (d) average December and January SST (increased Cabo Frio upwelling). The polygon represents the location of the CFUS mud facies, and the white dotted line represents the continental shelf break.

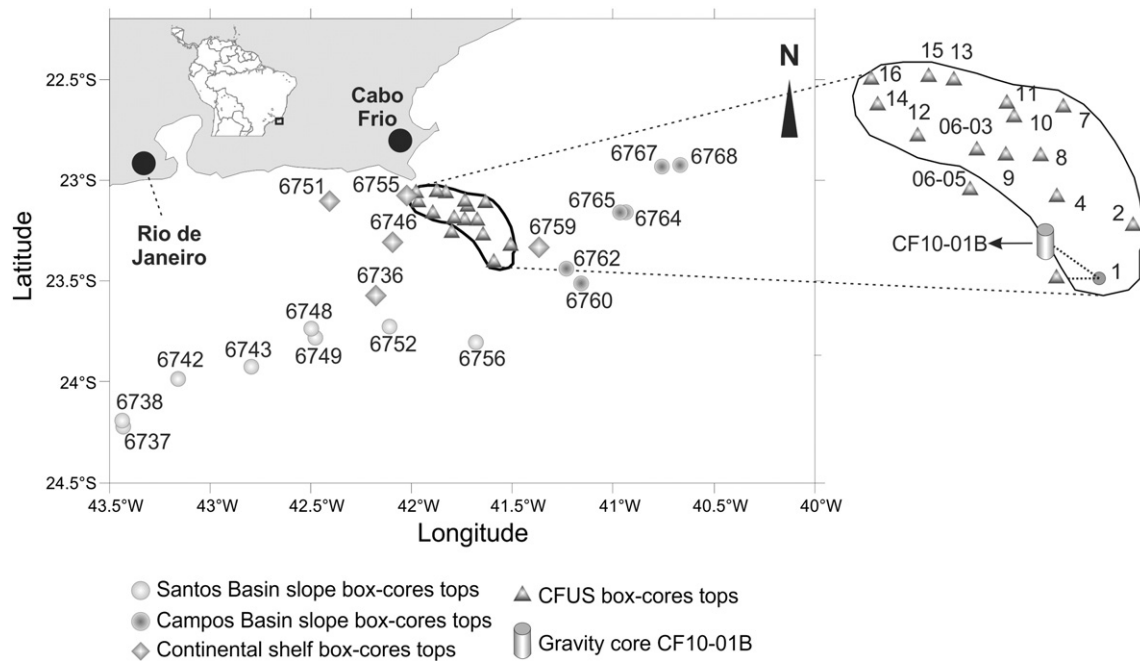


**Fig. 3.** Location of the RJCM and sampling points. Circles indicate continental slope REVIZEE box-core tops; diamonds indicate continental shelf REVIZEE box-cores tops; and triangles indicate CFUS box-core tops from the Ressurgência and CLIMPAST projects. Site 1 (gray circle) was sampled using a box-core and the CF10-01B gravity core.

deposit. We defined biofacies in this study using planktonic foraminifers. The core was subsampled at 1 cm intervals along its length, and 20 organic matter samples were dated using  $^{14}\text{C}$  acceleration mass spectrometry (AMS) in the Beta Analytic laboratory. The calibration of radiocarbon ages and the chronological model were carried out using Clam

software (Blaauw, 2010), with the Marine09 curve (Reimer et al., 2009) and a  $\Delta R$  of  $8 \pm 17$  years, as described by Angulo et al. (2005). The chronological model was constructed using a smoothing spline function, including mixed effects, with 1000 interactions and exclusion of curves with negative sedimentation rates by the software.

For micropaleontological analysis,  $10\text{ cm}^3$  of the sediment was washed through a  $125\ \mu\text{m}$  mesh sieve. The residue was dried at  $50\ ^\circ\text{C}$  and subjected to planktonic foraminiferal analysis, in which 300–500 specimens per sample were identified at the species level (Kennett and Srinivasam, 1983; Loeblich and Tappan, 1988). To normalize the species concentration data from the  $> 125\ \mu\text{m}$  sieve, the census counts were converted to the number of tests per  $\text{cm}^3$ . The morphotypes of *Globigerinoides sacculifer*, with and without a sac, were treated as a single species (*G. sacculifer*), as were the pink and white morphotypes of *Globigerinoides ruber* and the species *Globorotalia menardii*, *Globorotalia tumida* and *Globorotalia unguata* (here referred to as *G. menardii* plexus). The *G. ruber* morphotypes were not differentiated because sampling in the Santos Basin was conducted to allow the identification of living benthic foraminifera; therefore, rose Bengal staining was used. A total foraminifera census count will be stored in the [www.pangaea.de](http://www.pangaea.de) world database.

The *Globigerina bulloides*/*G. ruber* ratio (Gb/Gr) (Tolderlund and Bé, 1971; Kucera, 2007; Toledo et al., 2008; Souto et al., 2011), cold/warm species ratio (C/W) and MAT method (see Section 3.3) were employed to reconstruct the upwelling intensity and temperatures, respectively. The C/W ratio was based on integration of species preferences as described by Lidz (1966) and Kucera (2007).

### 3.2. Biofacies model

The biofacies model was developed using Primer 6 and Statistica 7 software (using the Ward distance measure). The data on the absolute abundance of planktonic foraminifera (tests  $\cdot\text{cm}^{-3}$ ) from the thirty-four box-core tops were introduced and transformed into relative abundance data (%). Bray–Curtis dissimilarity was applied in a Q-mode cluster analysis and in multidimensional scaling (MDS, Kruskal, 1964). The groups were compared by site and distance and were considered to be biofacies factors.

**Table 1**  
Box-core collection sites, including the latitude, longitude and water depth, in the RJCM.

Core id.	Latitude	Longitude	Water depth (m)	Location
BCCF10-16B2	–23.071	–41.981	103	CFUS
BCCF10-15A1	–23.059	–41.876	79	CFUS
BCCF10-14B1	–23.110	–41.967	113	CFUS
BCCF10-13A2	–23.065	–41.832	82	CFUS
BCCF10-12B3	–23.164	–41.894	121	CFUS
BCCF10-11B3	–23.105	–41.736	96	CFUS
BCCF10-10A2	–23.128	–41.720	101	CFUS
BCCF10-09B2	–23.201	–41.736	117	CFUS
BCCF10-08A1	–23.198	–41.675	113	CFUS
BCCF10-07A3	–23.112	–41.635	93	CFUS
BCCF10-04A2	–23.276	–41.645	120	CFUS
BCCF10-02B3	–23.325	–41.508	119	CFUS
BCCF10-01B1	–23.404	–41.590	128	CFUS
BCCF06-03	–23.190	–41.790	117	CFUS
BCCF06-05	–23.260	–41.800	124	CFUS
6736	–23.573	–42.176	103	Santos Basin (shelf)
6737	–24.223	–43.432	476	Santos Basin (slope)
6738	–24.193	–43.437	330	Santos Basin (slope)
6742	–23.986	–43.158	215	Santos Basin (slope)
6743	–23.923	–42.793	508	Santos Basin (slope)
6746	–23.308	–42.095	100	Santos Basin (shelf)
6748	–23.782	–42.478	497	Santos Basin (slope)
6749	–23.737	–42.497	325	Santos Basin (slope)
6751	–23.103	–42.407	93	Santos Basin (shelf)
6752	–23.727	–42.108	502	Santos Basin (slope)
6755	–23.077	–42.023	104	CFUS
6756	–23.804	–41.679	650	Cabo Frio High
6759	–23.333	–41.367	110	Campos Basin (shelf)
6760	–23.513	–41.158	419	Campos Basin (slope)
6762	–23.439	–41.231	146	Campos Basin (slope)
6764	–23.159	–40.937	425	Campos Basin (slope)
6765	–23.159	–40.950	246	Campos Basin (slope)
6767	–22.934	–40.757	453	Campos Basin (slope)
6768	–22.926	–40.668	280	Campos Basin (slope)

Cluster and MDS analyses are recommended, but not obligatory. Grouping data according to either regions or water masses would be sufficient, but multivariate analysis can improve the consistency of the groups obtained and provide a clear oceanographic context for each group. In our study area, this procedure was necessary because of a lack of data related to the local oceanography and planktonic foraminiferal assemblages. In areas where the oceanographic and planktonic foraminiferal community structures are well known, cluster analyses would be less important.

The biofacies similarity was analyzed according to analysis of similarity (ANOSIM) and the similarity percentage (SIMPER, Clarke, 1993) as a mean value of (dis)similarity. The ANOSIM and SIMPER analyses were applied to identify significant differences and to reveal the level of coherence of the planktonic foraminiferal assemblages related to the biofacies, respectively (indicated by intra-factor similarity values). High values imply similar biofacies, whereas lower values indicate that biofacies consist of samples with very different faunas. SIMPER analysis is particularly effective because it identifies the foraminiferal biofacies that can be related to oceanographic information and measures how fossil assemblages are similar to the obtained biofacies.

After obtaining the biofacies, the dissimilarities from the fossil assemblages in the gravity core CF10-01B were calculated. This step was also conducted via SIMPER analysis by calculating the average relative abundance in the biofacies. Hence, a dissimilarity value (also a percentage) is calculated based on the ranking of the species. Dissimilarity values were converted to similarity values by subtracting 100 from the obtained values. Only dissimilarity values between biofacies and fossil data were recovered and used to reconstruct past variability.

In summary, this biofacies model generates a calibration using modern analogs for different oceanographic settings to apply to the fossil record and to reconstruct the local/regional paleoceanography (the geographic range of the reconstruction depends on the geographic coverage of the recent assemblage databank). The model incorporates and analyzes all species (all specimens in the assemblage must be identified), but SIMPER analysis prioritizes the more abundant species; thus, rare species have very little influence on the model. The model, therefore, takes into account the whole vertical community structure, reducing the bias from shallow- and deep-dwelling species that is observed in transfer function methods (Kucera et al., 2005).

Alternatively, the model is weak in reconstructing paleoceanographic characteristics if the fossil assemblages are too dissimilar from modern assemblages (a non-analog situation), producing less reliable results, as commonly occurs when reconstructing glacial conditions.

### 3.3. MAT method

The MAT applied for the reconstruction of SST was performed with C2 data analysis software using the South Atlantic database from Niebler and Gersonde (1998) (SA model). This database includes 81 core tops collected between latitudes of 24°S and 55°S and longitudes of 80°W and 15°E. The size class of the quantified assemblage of planktonic foraminifera described in this database was the same as in the present study (>125 µm). A second reconstruction was performed based on the Niebler and Gersonde (1998) database and additional 34 box-core tops investigated in this study, totaling 115 samples (SA + RJCM model). The SST for each box-core top represents the average of an eight-year time series obtained from the MODIS on Aqua database, downloaded on August 2011 (<http://las.pfeg.noaa.gov/oceanWatch/oceanwatch.php>) on (Fig. 2).

The performance of the models (SA and SA + RJCM) was tested using the leave-one-out cross-validation method, and dissimilarities were calculated using the weighted Square Chord matrix method. The model errors were expressed as the Root Mean Square Error of Prediction (RMSEP). The reconstructed SST for core CF10-01B was based on the average SST from the 10 best analogs.

## 4. Results

Among the twenty-nine species identified, *G. ruber* was the most abundant, showing percentages between 26% (box-core top BCCF06-03, CFUS) and 73% (box-core top 6760, Campos Basin, Table 2). The percentage of *G. bulloides* ranged from 1% (6765, Campos Basin slope) to 19% (BCCF10-07A3, CFUS); *Globigerinita glutinata*, from 3% (BCCF10-07A3, CFUS) to 33% (6737, Santos Basin slope); and *Globoturborotalita rubescens*, from 1.7% (6756, Santos/Campos boundary's slope) to 20% (BCCF06-05, CFUS); *Turborotalita quinqueloba* showed percentages of up to 10% (BCCF10-12C3, CFUS); *Globigerinella calida*, of up to 7.5% (BCCF10-04A2, CFUS); *G. sacculifer*, of up to 6.3% (Santos Basin slope); and the percentage of *G. menardii* plexus ranged from 0.2% (BCCF10-14B1, CFUS) to 6.5% (6765, Santos Basin's slope).

The assemblages from the Campos Basin were marked by higher percentages of warm and oligotrophic taxa, such as *G. ruber*, *G. sacculifer*, *Globorotalia truncatulinoides* and *G. menardii* plexus (Fig. 4). The Santos Basin was characterized by higher percentages of *G. glutinata*, *G. rubescens* (on the shelf) and *Globigerinella siphonifera*. In the CFUS, the cold-water species *G. bulloides* and *T. quinqueloba*, *G. rubescens*, *G. glutinata* and *G. calida* were present in the highest percentages. Taking into account the comparison between the neritic and oceanic species distributions, the taxa *G. ruber*, *G. sacculifer*, *G. menardii* plexus and *G. truncatulinoides* were more abundant on the continental slope, whereas *G. bulloides*, *T. quinqueloba*, *G. calida*, *G. glutinata* and, particularly, *G. rubescens* were more abundant over the continental shelf.

The MDS and cluster analysis separated the 34 box-core tops into four main groups (Fig. 5a and b), which were mapped with considerable geographical separation (Fig. 5c). ANOSIM (Table 3) indicated significant differences among the groups, characterizing the occurrence of four biofacies in the RJCM. Biofacies A comprises the box-core tops from the Campos Basin, while biofacies B includes the box-core tops collected on the continental shelf and on the slope of the Santos Basin. The CFUS was divided into two biofacies: the Northern CFUS was defined as biofacies C, and the Southern CFUS was defined as biofacies D. Despite sharing the same ecosystem, i.e., the Cabo Frio upwelling system, biofacies C and D were more similar to the Campos and Santos biofacies, respectively, than to each other (Fig. 5).

With respect to core CF10-01B, <sup>14</sup>C dating indicated a time range of 11.5 cal kyr (Table 4, Fig. 6), with larger uncertainty in the ages between 382 cm (the bottom of the core) and 230 cm. This layer consists of a loamy sand facies, representative of a marine transgression when erosion and sedimentary reworking were most likely common. Because of the high incidence of reversed ages, this core section was not discussed in this manuscript. From a core depth of 230 cm to the top of the core, the sediment consists of organic clay.

The variations in the planktonic foraminiferal percentages in core CF10-01B were similar to those found in recent assemblages, with few exceptions (Fig. 7). The most abundant taxa were *G. ruber* (35–55%), *G. bulloides* (5–20%), *G. glutinata* (5–20%), *G. rubescens* (5–25%), *T. quinqueloba* (1–12%), *G. calida* (3–10%), *G. sacculifer* (0.5–5%) and *G. menardii* plexus (0–2.5%).

The percentage of *G. bulloides* was high prior to 6.0 cal ka BP and after 2.5 cal ka BP (approximately 15%), while the lowest percentages of this species were found between 3.5 and 2.5 cal kyr BP (approximately 5%). The percentage of *T. quinqueloba* was below 5% prior to 2.0 cal ka BP and increased to more than 10% from 1.5 cal ka BP to the top of the core. The percentage of *G. ruber* varied from 45% to 55%, with the highest values being found between 7 and 5 cal kyr BP and between 3.5 and 2.5 cal kyr BP, which was synchronic with the abundance of other species of the Campos Basin. However, *G. sacculifer* was an exception, with an abundance ranging from 4% to 8% before cal 6 cal ka BP and from 1% and 2% after this time. The percentage of *G. glutinata* was lower (less than 10%) prior to 6 cal ka BP, increasing to more than 12% after 6 cal ka BP, and displaying peaks of 18–20%

**Table 2**  
Relative abundance of the main planktonic foraminifera species in the box-core tops from the RJCM.

Core id.	Planktonic foraminifera relative abundance (%)													
	<i>O. universa</i>	<i>G. ruber</i> (total)	<i>G. tenella</i>	<i>G. sacculifer</i> (total)	<i>G. siphonifera</i>	<i>G. calida</i>	<i>G. bulloides</i>	<i>G. rubescens</i>	<i>T. quinqueloba</i>	<i>N. dutertrei</i>	<i>G. glutinata</i>	<i>G. conglobatus</i>	<i>G. menardii</i> plexus (total)	<i>G. truncatulinoides</i>
BCCF10-16B2	0.96	58.47	0.32	2.24	1.28	5.43	15.97	5.43	2.88	0.96	4.79	0.00	0.96	0.00
BCCF10-15A1	0.60	53.27	1.49	3.27	0.30	4.76	11.90	10.71	3.57	0.89	8.93	0.00	0.30	0.00
BCCF10-14B1	0.80	37.02	1.21	1.41	0.20	2.82	17.71	13.08	7.04	0.20	16.10	0.20	0.20	0.20
BCCF10-13A2	0.91	45.12	0.61	1.52	0.30	6.40	10.98	16.46	6.10	0.00	8.84	0.00	0.91	0.00
BCCF10-12B3	0.39	30.10	1.55	0.97	0.19	5.63	11.26	18.45	9.71	0.58	19.42	0.39	0.58	0.19
BCCF10-11B3	0.34	50.17	1.69	1.69	0.68	5.42	13.22	7.12	6.10	0.68	8.47	1.02	2.71	0.34
BCCF10-10A2	0.37	43.07	1.87	3.37	1.87	3.75	16.48	13.86	6.37	0.75	5.62	0.37	1.12	0.37
BCCF10-09B2	1.15	33.85	1.15	1.54	0.77	3.46	11.54	11.54	9.62	0.00	23.46	0.38	0.38	0.00
BCCF10-08A1	0.75	43.66	0.37	1.12	0.75	5.60	13.81	10.45	6.72	0.75	13.43	1.12	0.37	0.00
BCCF10-07A3	0.31	47.80	1.26	2.83	0.63	5.35	19.18	10.69	6.60	0.63	3.14	0.31	0.94	0.00
BCCF10-04A2	0.34	38.05	1.68	2.02	1.01	7.41	12.12	10.77	9.09	0.00	15.49	0.34	1.68	0.00
BCCF10-02B3	0.47	57.08	1.89	2.83	1.18	2.59	12.74	10.85	2.83	0.24	4.25	0.47	2.12	0.24
BCCF10-01B1	0.00	33.41	2.86	1.32	0.66	6.37	9.89	20.00	9.67	0.00	13.41	0.00	1.32	0.22
BCCF06-03	0.45	26.40	1.07	0.36	0.71	5.00	17.84	14.27	9.63	0.71	18.55	0.00	1.07	0.00
BCCF06-05	0.02	32.24	1.09	0.47	0.31	6.54	11.68	20.09	4.05	0.00	20.25	0.16	1.09	0.00
6736	0.00	54.74	0.00	0.00	2.11	2.11	9.47	18.95	0.00	4.21	6.32	1.05	1.05	0.00
6737	0.00	38.59	0.00	0.33	1.81	3.78	5.58	13.63	0.16	0.33	33.17	0.33	0.66	0.00
6738	0.50	41.79	0.50	2.49	1.74	1.74	4.98	15.67	0.25	1.24	24.63	0.75	1.00	0.75
6742	0.00	59.64	1.43	3.21	2.50	0.71	8.21	7.50	0.36	1.79	10.36	0.71	0.36	1.07
6743	0.30	49.26	0.00	4.15	2.08	2.67	3.26	16.32	0.00	0.89	18.40	0.59	0.59	0.89
6746	0.00	47.92	0.57	1.13	2.26	3.21	2.64	13.77	1.13	0.57	22.45	0.94	1.13	0.00
6748	1.36	45.58	0.68	3.06	3.40	1.02	3.74	9.52	0.68	1.02	26.87	1.02	0.34	1.02
6749	0.00	31.30	1.22	2.20	6.60	3.18	8.56	13.94	0.24	0.49	30.32	0.00	0.49	0.49
6751	0.00	32.61	0.00	0.39	2.16	1.57	9.82	17.09	4.13	1.18	28.29	0.39	0.79	0.39
6752	1.35	44.61	0.60	6.29	1.65	1.35	5.39	11.83	0.90	0.90	20.51	0.90	1.80	0.30
6755	0.00	33.52	0.00	0.57	1.70	0.85	6.53	17.61	8.52	2.27	26.70	0.28	0.57	0.00
6756	2.22	72.06	0.22	5.32	2.22	0.67	3.77	1.77	0.00	0.89	6.65	1.11	2.44	0.44
6759	0.00	59.02	0.00	1.64	0.60	1.34	7.75	18.03	1.04	0.89	8.64	0.30	0.75	0.00
6760	0.83	73.76	0.28	4.42	0.83	1.10	4.42	4.70	0.00	0.00	4.14	0.55	2.21	1.93
6762	0.45	71.27	0.00	3.34	1.78	0.45	4.45	4.68	0.45	0.89	7.57	0.67	2.45	1.56
6764	0.00	67.02	0.15	2.56	1.66	2.11	2.26	7.53	0.60	0.90	10.24	0.45	2.26	1.20
6765	0.36	63.50	0.36	6.20	1.09	0.00	1.46	4.38	0.36	3.28	5.47	4.01	6.57	2.19
6767	0.26	41.86	0.26	0.65	2.97	2.58	4.01	12.27	2.84	1.42	31.65	0.39	1.94	0.26
6768	0.29	73.07	0.00	3.44	0.86	1.43	2.58	4.01	0.00	0.29	8.60	1.72	2.58	0.86

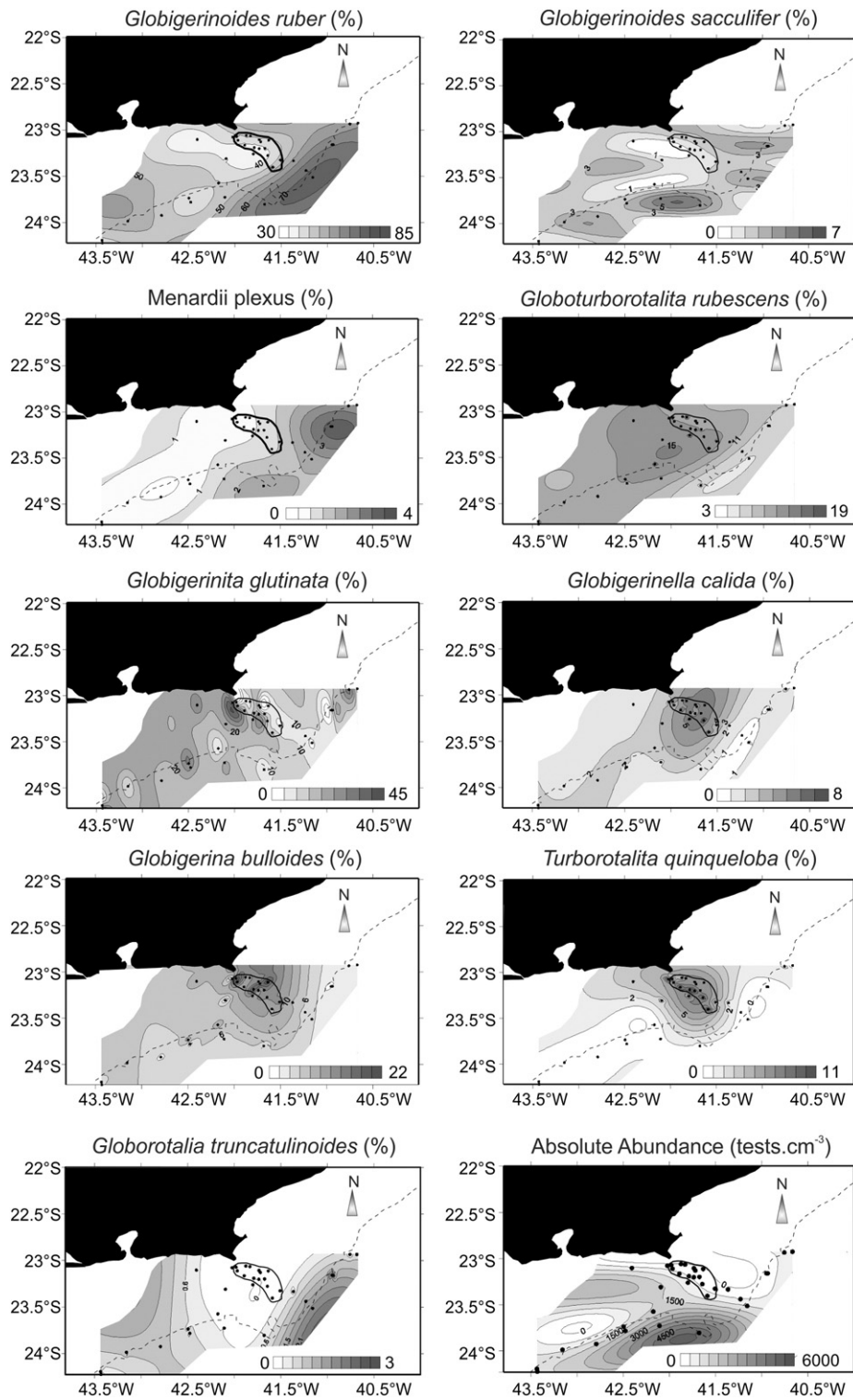
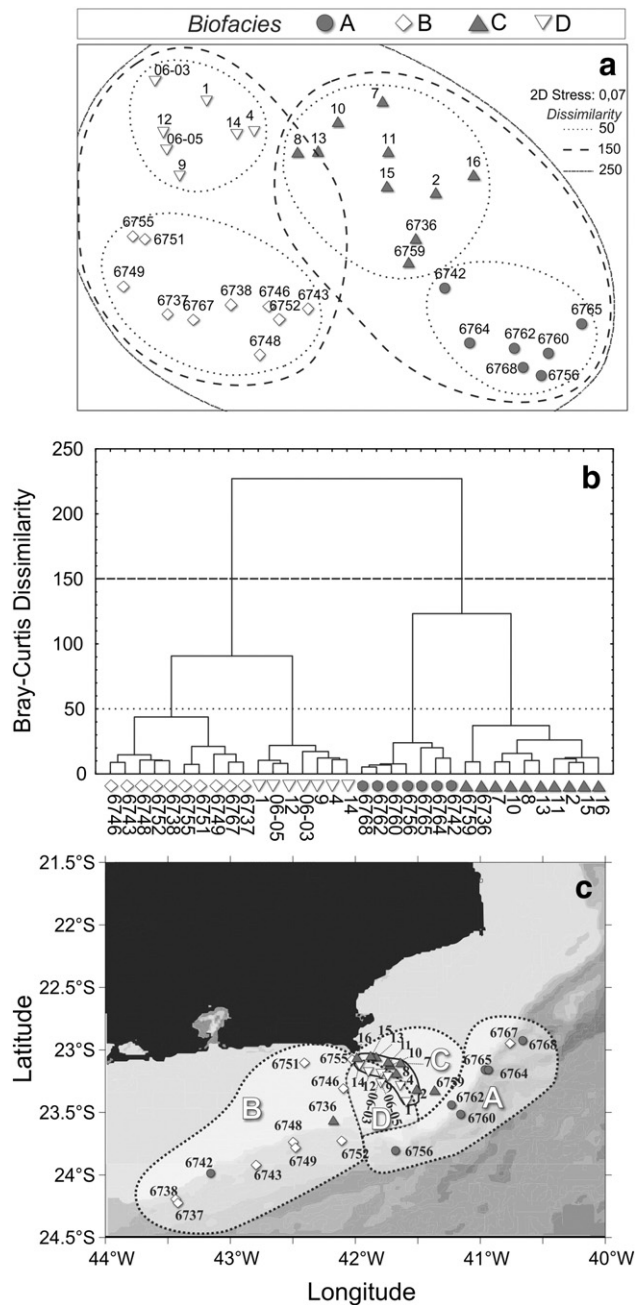


Fig. 4. Distribution of the total absolute abundance and the relative abundances of the total absolute abundance and the main planktonic foraminifera species among box-core tops in the RJCM.

2.0 cal ka BP. The species *G. rubescens* presented its highest abundance (approximately 20–25%) prior to 7.5 cal ka BP and at approximately 4 cal ka BP and showed its lowest percentages (5% and 15%) from approximately 6.2–5.5 cal kyr BP and 2–1.5 cal kyr BP. Trace amounts of thermocline species (*G. truncatulinoides*, *Globorotalia inflata*, *Globorotalia hirsuta* and *Globorotalia crassaformis*) occurred during the considered time range. However, the percentages of these thermocline species reached up to 3% in the lowermost 150 cm (section excluded).

The Gb/Gr and C/W ratios presented similar variations along core CF10-01B: a cold period was observed between 9.0 and 6.0 cal kyr BP; a warm period between 6 and 2.5 cal kyr BP, with a cold, short event detected between 4.0 and 3.5 cal kyr BP; and the return of a cold period for the last 2.5 cal kyr. However, the two ratios yielded contradictory indications of the intensity of these events: the Gb/Gr ratio identified the period between 3.5 and 2.5 cal kyr BP (after the 4.0–3.5 cal kyr BP cold event) as the warmest period, whereas the C/W



**Fig. 5.** Grouping analysis results for the RJCM planktonic foraminiferal assemblages. (a) MDS analysis, (b) cluster analysis and (c) geographic distribution of biofacies.

ratio identified the period between 6.0 and 2.5 cal kyr BP as the warmest period, with no intensity differences being observed before or after the 4.0–3.5 cal kyr BP cold event (Fig. 8).

The MAT SA + RJCM model performed slightly better than the SA model (Table 5). The SST reconstructions produced larger standard deviations in the SA model than in the SA + RJCM model as well as larger

dissimilarity values from the fossil assemblages. The slightly better performance of the SA + RJCM model compared to the SA model was expected because the examined core is located in the RJCM and therefore tended to use the SST values from RJCM core tops due to the high similarities. The range of variability in the SSTs reconstructed by the MAT was approximately 0.35 °C along the core (Fig. 8), indicating no SST variability during the Holocene, as this SST range is lower than the model's RMSEP (Table 5). Despite the small SST variation in the core, different phases could be identified. Cold SSTs were identified between 9.0 and 5.0 cal kyr BP, with a minimum SST being detected between 7.2 and 6.0 cal kyr BP, which was indicated only by the SA + RJCM model. Warm SSTs predominated between 5.0 and 2.0 cal kyr BP, during which a slight cold period was observed, for which the two models produced contrasting results: the SA model indicated dominance of southern upwelling (4.0–3.5 cal kyr BP, Fig. 8), whereas the SA + RJCM model indicated a longer time span during which southern upwelling increased (4.5–3.5 cal kyr BP, Fig. 9). Between 3.5 and 2.0 cal kyr BP, the two reconstructions were in agreement, indicating warm SSTs. After 2.0 cal ka BP, the two reconstructions were contradictory, with the SA model indicating high SSTs until 1.5 cal ka BP, with a cooling trend being observed thereafter, and the SA + RJCM model indicated a cooling trend after 2.5 cal ka BP, with cold SSTs occurring after 2.0 cal ka BP.

## 5. Discussion

### 5.1. Ecological and oceanographic context of the planktonic foraminifera distribution in the RJCM

The ecology and distribution of planktonic foraminifera were defined according to the site where the species abundance was highest based on oceanographic conditions.

The occurrence of *G. ruber*, *G. sacculifer* and *G. menardii* plexus in warm and oligotrophic waters is well documented. These taxa are typical in the Brazil Current and in the Subtropical Gyre because *G. ruber* and *G. sacculifer* are surface dwellers where the water is clear and because *G. menardii* plexus inhabits subsurface waters where chlorophyll-*a* levels are elevated (Bé, 1977; Raveloet et al., 1990; Niebler et al., 1999; Schmuker and Schiebel, 2002; Coloma et al., 2005; Ding et al., 2006; Martinez et al., 2007). These species are distributed along the Brazilian continental margin near the front of the Brazil Current (Boltovskoy et al., 1996). In the present study, these species were mainly found to be distributed among the offshore core tops, particularly in those on the Campos Basin slope (Fig. 4). Therefore, this species group could be related to an oligotrophic water column.

With respect to the distribution of foraminifera in the South Atlantic subsurface layer (below a depth of 100 m), there was a predominance of *G. menardii* plexus, while low abundances of *G. crassaformis* and *G. hirsuta* were observed at tropical and subtropical latitudes (in the Subtropical Gyre). These species are replaced by *G. inflata*, *G. truncatulinoides* and *Globorotalia scitula* in transitional and subantarctic latitudes (Boltovskoy et al., 1996; Niebler et al., 1999). Specimens of *G. truncatulinoides* can also be found in subtropical waters, but at low abundances, generally displaying the right-coiling form, whereas the specimens found in transitional and subantarctic waters generally present the left-coiling form (Niebler et al., 1999). However, in Cabo

**Table 3**  
ANOSIM results for the four biofacies.

Biofacies	Statistic	R significance level %	Possible permutations	Actual permutations	No. $\geq$ observed
C $\times$ D	0.797	0.1	19448	999	0
B $\times$ C	0.93	0.1	92378	999	0
A $\times$ C	0.871	0.1	19448	999	0
B $\times$ D	0.825	0.2	19448	999	1
A $\times$ D	1	0.1	1716	999	0
A $\times$ B	0.988	0.1	19448	999	0

**Table 4**  
Radiocarbon and calibrated ages generated by Clam software for core CF10-01B.

Material	Depth (cm)	Code	Age <sup>14</sup> C (ka BP)	Uncertainty (years)	Calibrated age 95% interval (ka)		
					Minimum	Maximum	Probability
Organic matter	1	AA93441	1.03	36	0.53	0.66	95
	10	AA90740	1.91	39	1.35	1.54	95
	20	AA93442	1.72	38	1.18	1.34	95
	40	AA89728	2.96	48	2.61	2.84	95
	70	AA93443	3.22	37	2.89	3.15	95
	80	AA90736	3.45	41	3.20	3.41	95
	100	AA93444	3.92	38	3.78	3.78	0.3
					3.79	4.04	94.7
	130	AA93445	4.06	39	3.95	4.21	95
	140	AA90738	4.94	44	5.08	5.09	0.9
					5.11	5.43	94.1
	160	AA93446	5.16	40	5.43	5.59	95
	170	AA93447	5.73	41	6.01	6.25	95
	200	AA90734	6.99	48	7.41	7.57	95
	210	AA93448	6.59	43	6.99	7.22	95
	230	AA93449	8.80	48	9.38	9.54	95
	250	AA89729 <sup>a</sup>	10.07	59	10.80	10.86	4.1
					10.88	11.19	90.9
	300	AA90735	9.26	56	9.90	10.20	95
	330	AA93450	8.96	58	9.49	9.81	95
	340	AA90739	9.05	67	9.53	9.97	93.4
					9.97	10.00	1.6
360	AA93451	9.27	50	9.92	10.21	95	
370	AA89730	11.13	110	12.38	12.88	95	

<sup>a</sup> Date not used in the age model.

Frio, no coiling preference could be observed, most likely due to the mixture of water masses. Vicalvi (1997) and Portilho-Ramos et al. (2006) reported the disappearance of *G. menardii* plexus and increases in the percentages of *G. truncatulinoides* and *G. inflata* in glacial sediments in the southeastern and southern Brazilian continental margins, respectively. These species were classified as traces (rare occurrences) in recent sediments (except for *G. truncatulinoides*, which reached 1.5% in sediment on the Campos Basin slope, Fig. 4).

*G. glutinata* is a subtropical species that is not dependent on temperature, salinity or depth. It is sensitive to changes in productivity,

especially to diatom blooms (Boltovskoy, 1962; Bé, 1977; Kennett and Srinivasam, 1983; Eguchi et al., 1999; Schmuker and Schiebel, 2002; Ding et al., 2006; Machain-Castillo et al., 2008). Schmuker and Schiebel (2002) found high abundances of *G. glutinata* in the center of cyclonic eddies in the Caribbean Sea. These eddies are known for bringing nutrient-rich waters into the photic zone, leading to the formation of a zone of high productivity. In the present study, the percentage of *G. glutinata* was higher in the sediment of the Santos Basin on both the continental shelf and slope (Fig. 3), where meanders and eddies are frequent because of the mixing of water masses (Calado et al., 2006; Belem et al., 2013).

The species *G. siphonifera* and *G. calida* are associated with subtropical waters. These species bear symbionts and often feed on zooplankton, allowing them to occupy waters with low nutrient availability and even the sea-sediment layer (Schmuker and Schiebel, 2002). In this study, the occurrence of these bioindicators in the Santos Basin characterized this basin as harboring warm/oligotrophic and productive water. Oceanographic variability is high in the Santos Basin because of the instability of the Brazil Current and the coastal water input, particularly the input from Guanabara Bay. The species *G. calida* was also found at a high abundance, above 5%, in the CFUS, indicating a connection with upwelling productivity. Because *G. calida* is not typically described as an inhabitant of upwelling areas, this species could take advantage of short upwelling events. In this context, *G. calida* might proliferate during a late upwelling planktonic bloom under warm water conditions, where it could actively feed on zooplankton or marine snow.

*G. rubescens* shows a tropical-subtropical distribution (Kennett and Srinivasam, 1983), but its ecological preferences are poorly known, possibly because of its small size (Al-Sabouni et al., 2007). This species was observed near the shelf in the northeast African margin (Bé and Hamlin, 1967) and in the southeast Brazilian margin (MARGO database, Pflaumann et al., 1996). In this study, we found *G. rubescens* to be one of the most abundant species in the assemblages of the RJCM, presenting percentages ranging from 5% to 20% (Fig. 4). The highest percentages of *G. rubescens* (above 15%) in the study area were found over the continental shelf (on the inner shelf and offshore from the CFUS), where *G. rubescens* was considered an indicator of neritic waters. The low percentage of *G. rubescens* observed on the inner shelf of the CFUS compared with the rest of the shelf could be associated with upwelling,

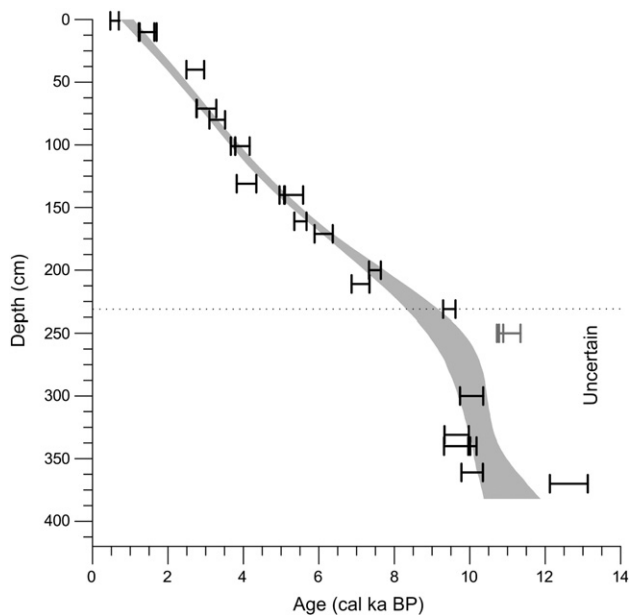


**Fig. 6.** Chronological model built using Clam software for core CF10-01B. Error bars represent the 95% confidence interval of the calibration curves for the age uncertainty, and the gray area represents the uncertainty of the smoothing spline function interpolation. The gray error bar represents the dating point excluded from the chronological model. The dotted line separates the core sections that were included and excluded for paleoenvironmental interpretations.

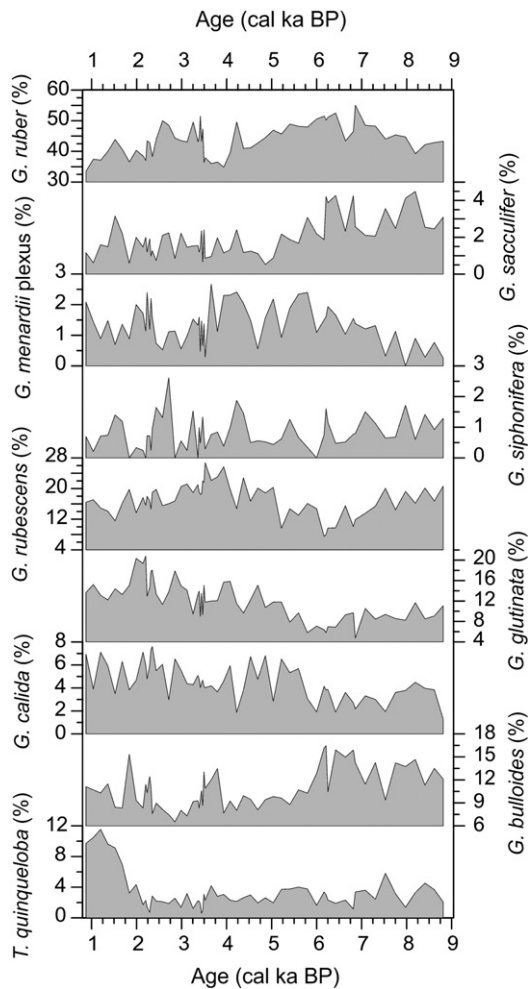


Fig. 7. Variability of the relative abundance of the main planktonic foraminifera species along core CF10-01B. "Globorotalia menardii plexus" includes *Globorotalia menardii*, *G. tumida* and *G. unglata*.

which favors the predominance of cold-water species, decreasing the relative abundance of *G. rubescens*.

The cold-water species *Globigerina bulloides* and *T. quinqueloba* are abundant south of the Atlantic Subtropical Gyre (35°S) under the influence of the Malvinas Current (Boltovskoy, 1962; Boltovskoy et al., 1996). However, *G. bulloides* is also found in high abundance in upwelling areas, in contrast with *T. quinqueloba*, which is not very prevalent in the tropics (Kucera, 2007). The latter species is typically abundant in cold and very productive waters and usually inhabits the surface layer (Boltovskoy et al., 1996; Coloma et al., 2005; Ding et al., 2006; Naidu, 2007; Rasmussen and Thomsen, 2011). In the present study, both species were found to be abundant in the CFUS (Fig. 4), but the highest abundance of *G. bulloides* was found in the northern CFUS, whereas the highest abundances of *T. quinqueloba* were observed in the southern and western CFUS. Therefore, the two species were treated as cold water indicators, with *T. quinqueloba* being linked to colder water than *G. bulloides*.

## 5.2. Oceanographic characterization of the biofacies

Biofacies A could be associated with the warm and oligotrophic water of the Brazil Current related to the Campos Basin slope (Table 6). There was a large contribution of *G. ruber* (76%) in biofacies A, in which species such as *G. glutinata*, *G. rubescens* and *G. bulloides* contributed less than 7%. The remaining 95% of the biofacies was contributed by the Tropical Water taxa *G. menardii plexus* and *G. sacculifer*.

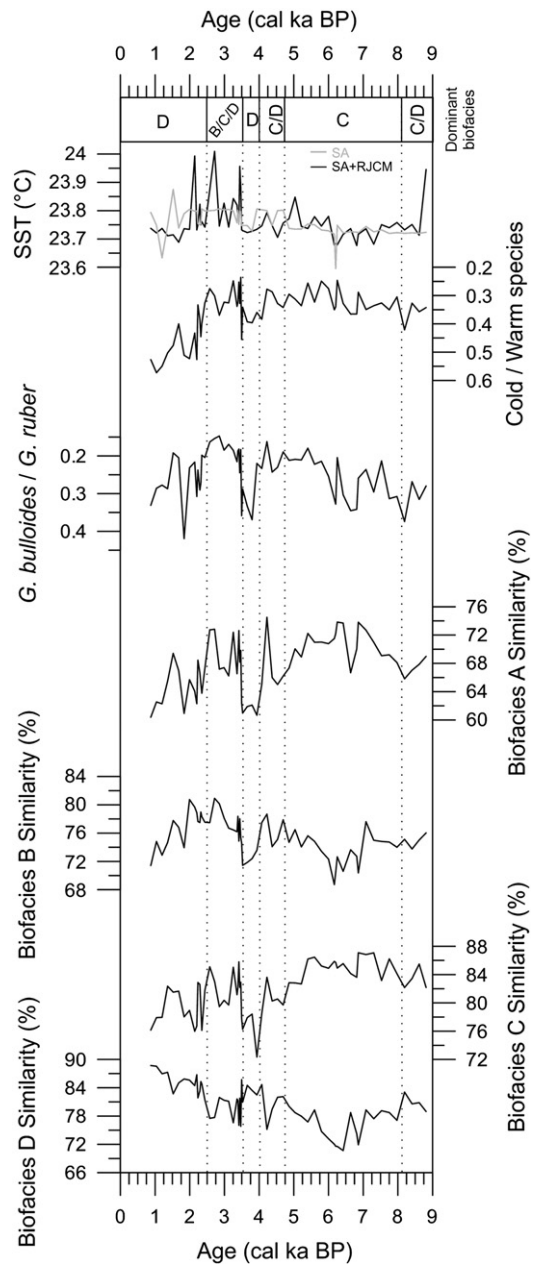


Fig. 8. Comparison of the biofacies variability, abundance ratios of planktonic foraminifera species and SST reconstructions along core CF10-01B.

In biofacies B, the contribution of *G. ruber* was lower than in biofacies A, and shelf species that serve as indicators of productivity, such as *G. glutinata* and *G. rubescens*, together with *G. ruber*, accounted for 85% of the contribution in this biofacies. Therefore, biofacies B is representative of a mixed water mass with a strong coastal and estuarine influence (Guanabara Bay), showing a high nutrient concentration and small contribution of Cabo Frio upwelling that could be related to warm and productive waters (coastal and oceanic waters).

Biofacies C included 53% *G. ruber*, cold-water species such as *G. bulloides* and *T. quinqueloba*, the shelf species *G. rubescens* and the subtropical species *G. calida*. This biofacies represents attenuated or induced local upwelling conditions in the northern half of the CFUS, and because of the Brazil Current and northern Rio de Janeiro shelf water inputs, this biofacies may also include SACW upwelling plumes from Cabo de São Tomé (northern upwelling system).

Biofacies D represents the southern half of the CFUS, where the SACW upwelling coastal plume is located. It is characterized by a low

**Table 5**

Statistics for the MAT, showing the performance of the models (given by  $R^2$  and RMSEP), the average dissimilarities between the 10 best analogs and fossil assemblages, and the average standard deviation of SST reconstructions.

Database	$R^2$	RMSEP	Best analogs average dissimilarity	Average SD from SST ( $^{\circ}$ C)
South Atlantic (Niebler and Gersonde, 1998)	0.988	0.894	28.19–48.17	1.04
South Atlantic + RJC top cores	0.991	0.762	6.52–13.24	0.27

contribution of *G. ruber* (35%); high contributions of *G. glutinata*, *G. rubescens* and *G. bulloides*; a higher contribution of *T. quinqueloba* compared with biofacies C; and a low contribution of *G. calida*. Thus, this biofacies was linked to SACW cold-water upwelling conditions (southern upwelling system). It is important to emphasize that in this region, upwelling does not mean that SACW reaches the surface of the water column (sensu stricto upwelling); classic upwelling occurs only within 10 km of the coast (up to the 20 m isobath) (Albuquerque et al., in press). The southern upwelling system, expressed by biofacies D, indicates the presence of SACW in the photic zone due to the action of NE winds and wind stress curl, favoring increased productivity and the presence of cold-water foraminifera, displaying upwelling sensu lato.

### 5.3. CFUS biofacies separation

The separation of the assemblages within the Cabo Frio system demonstrates that the oceanographic characteristics of the Campos and Santos basins operate within the system, despite the occurrence of upwelling. The separation of the assemblages was determined by the Cabo Frio High, which separates the Campos and Santos basins.

The northern biofacies C faces the CFUS, in which the SST is generally higher than in the southern portion (Fig. 2a). This SST indicates a strong influence of Tropical Water, explaining the high percentages of *G. ruber* and *G. bulloides* and the low percentage of *T. quinqueloba*. In the southern CFUS, the shelf is deeper, and a low SST anomaly is found (Figs. 1c and 2), which could explain the decrease in the percentage of *G. ruber* and the increase in the percentages of cold-water species.

### 5.4. Sea-level fluctuations and dating reversals in core CF10-01B

Fig. 4 indicates that there were greater age uncertainties (approximately 800 years) in the first 150 cm of the core (11.5–9 cal kyr BP), representing sea-level fluctuations. The sedimentation of loamy sand

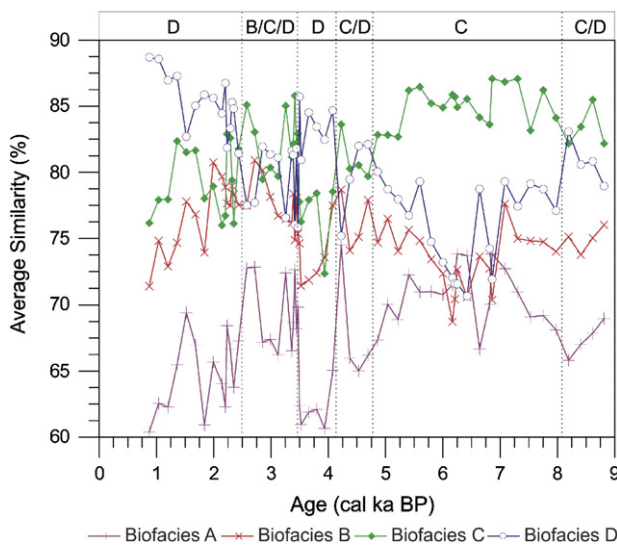


**Fig. 9.** Variability along core CF10-01B for the four biofacies, placed simultaneously in the same axis (ranked similarities): the Brazil Current front (biofacies A), mixing of shelf and oceanic waters (biofacies B), attenuated northern upwelling (biofacies C) and the intense southern upwelling (biofacies D). The dominant biofacies represents the main oceanographic scenario for the site.

during this time period could be attributed to a reworking during glacial regression. Based on the sea-level curves reported by Corrêa (1996) and Bard (1998), the sea level rose between 65 and 70 m from 11.5 to 7 cal kyr BP, when it reached its present level. This rise in sea level was not constant, and according to Corrêa (1996), the transgression accelerated dramatically after 9.5 cal ka BP, making the hydrodynamic regime on the shelf more pronounced. Such effects could have caused a strong reduction of the sedimentation rate, resulting in age reversals or gaps in the sedimentary record.

### 5.5. Application of the biofacies for paleoceanographic analyses

The defined biofacies were applied to core CF10-01B (site 1 in the CFUS, Figs. 3 and 5c) through a SIMPER analysis to determine the contribution of the biofacies to the defined paleoceanographic scenarios.

#### 5.5.1. Paleoceanographic diagnosis of the CFUS for the last 9000 years

The variability of the ranked similarities of the four recent biofacies along the core (Fig. 9) indicated that upwelling dominated at this site throughout the analyzed time period. From cal 9.0 to 6.0 cal kyr BP, a high similarity between the fossil assemblages and biofacies C was observed (Fig. 9), with a secondary increase in biofacies A being detected at 6.5 cal ka BP. This time period was characterized by northern upwelling conditions due to an intense influence of the Brazil Current. This scenario could be favored by a varying intensity of NE winds, promoting strong seasonal upwelling oscillations.

From 6 to 2.5 cal kyr BP, the biofacies C signal diminished, and the similarity increased between biofacies B and D, with this similarity becoming dominant after 5.0 cal ka BP. These two biofacies were correlated between 6 and 4 cal kyr BP but were anti-correlated after 4.0 cal ka BP. Between 4 and 3.5 cal kyr BP, the biofacies D scenario (southern upwelling) was dominant, while between 3.5 and 2.5 cal kyr BP, there was an alternation between biofacies C and D, with a strong biofacies B signal being observed, pointing to a weakening of the CFUS. This scenario implies a period during which coastal waters became more significant in determining the foraminiferal community structure in the CFUS. This period of coastal water input could have been caused by different sources of coastal water, including (1) the Holocene high stand between 6 and 4.5 cal kyr BP (Angulo and Lessa, 1997; Laslandes et al., 2005) and (2) increased precipitation over the continent between 4.5 and 2.5 cal kyr BP (Prado et al., 2012), enhancing the contribution of coastal waters from Guanabara Bay.

The period around 5.0 cal ka BP should be discussed in particular because several studies point to a strengthening of the South American monsoon after 5.0 cal kyr BP (Absy et al., 1991; Sifeddine et al., 2001; Turcq et al., 2002; Cruz et al., 2009; Razik et al., 2013). This strengthening of the monsoon could be responsible for the intensification of a continent–sea moisture corridor of intense precipitation (South Atlantic Convergence Zone, SACZ), which is considered to be the main source of moisture for SE Brazil, especially during the summer (Carvalho et al., 2004).

Prior to 5.0 cal ka BP, the latitudinal seasonal migration of the Intertropical Convergence Zone (ITCZ) presented a large seasonal latitudinal migration amplitude (Haug et al., 2001; Cruz et al., 2009). This ITCZ pattern generated an intensification of the winter and summer South Atlantic atmospheric conditions, resulting in weak NE winds and SACW upwelling during winter and strong NE winds and upwelling during summer. Such seasonal intensifications influenced the

**Table 6**  
SIMPER analysis results and diagnosis of the oceanographic setting for each biofacies.

Biofacies	Similarity (%)	Species	Av. Abund	Av. Similarity	Sim/SD	Contrib%	Cum.%	Oceanographic diagnosis		
A	89.19	<i>G. ruber</i>	70.15	67.77	18.16	75.98	75.98	Brazil Current front (warm and oligotrophic waters)		
		<i>G. glutinata</i>	7.12	5.76	3.92	6.46	82.44			
		<i>G. rubescens</i>	4.51	3.47	2.74	3.9	86.33			
		<i>G. sacculifer</i>	4.22	3.38	4.13	3.79	90.12			
		<i>G. bulloides</i>	3.16	2.4	2.55	2.69	92.81			
		<i>G. menardii</i> group	3.09	2.33	18.95	2.61	95.42			
		<i>G. ruber</i>	40.55	36.65	7.25	43.45	43.45			
		<i>G. glutinata</i>	26.17	23.38	6.23	27.73	71.18			
		<i>G. rubescens</i>	14.12	12.58	5.99	14.91	86.09			
		<i>G. bulloides</i>	5.44	4.09	3.14	4.85	90.94			
B	84.34	<i>G. siphonifera</i>	2.63	1.92	5.22	2.28	93.22	Mixture of shelf and oceanic waters (warm and productive waters)		
		<i>G. calida</i>	2.19	1.57	2.21	1.87	95.08			
		<i>G. ruber</i>	49.9	46.3	12.26	53.52	53.52			
		<i>G. bulloides</i>	14.3	12.7	8.29	14.67	68.2			
		<i>G. rubescens</i>	10.72	8.7	3.49	10.05	78.25			
		<i>G. glutinata</i>	7.2	5.22	2.58	6.04	84.29			
		<i>G. calida</i>	4.92	4.24	3.69	4.9	89.18			
		<i>T. quinqueloba</i>	5.15	4.19	2.67	4.84	94.02			
		<i>G. ruber</i>	33.09	30.69	9.59	35.47	35.47			
		<i>G. glutinata</i>	18.14	16.08	7.08	18.59	54.06			
C	86.51	<i>G. rubescens</i>	15.49	13.1	4.72	15.14	69.19	Attenuated or influenced upwelling by Brazil Current (northern upwelling, rather cold waters)		
		<i>G. bulloides</i>	13.18	11.39	6.84	13.17	82.36			
		<i>T. quinqueloba</i>	8.42	7.34	3.14	8.48	90.84			
		<i>G. calida</i>	5.33	4.32	3.15	4.99	95.83			
		D	86.52	<i>G. ruber</i>	33.09	30.69	9.59		35.47	Intense upwelling events (southern upwelling, cold waters)
				<i>G. glutinata</i>	18.14	16.08	7.08		18.59	
				<i>G. rubescens</i>	15.49	13.1	4.72		15.14	
				<i>G. bulloides</i>	13.18	11.39	6.84		13.17	
				<i>T. quinqueloba</i>	8.42	7.34	3.14		8.48	
				<i>G. calida</i>	5.33	4.32	3.15		4.99	

foraminiferal assemblages, which showed a strong correspondence with the northern upwelling condition.

After 5.0 cal ka BP, the amplitude of the seasonal migration of the ITCZ decreased in response to stronger summer Southern Hemisphere insolation. The result was a larger ocean–land temperature gradient, which favored migration of the low pressure zones from NE Brazil and enhancement of the South-American monsoon (Cruz et al., 2009) and, hence, of the SACZ (Prado et al., 2012). Thus, the incursion of Tropical Water tended to decrease, while that of shelf waters increased (biofacies B-like). Such explanations could be applied to interpret the variations in upwelling observed after 5.0 cal ka BP, with intense events occurring between 4.0 and 3.5 cal kyr BP and after 2.5 cal ka BP and weak events between 3.5 and 2.5 cal kyr BP. After 2.5 cal ka BP, the assemblages at the core site indicated current oceanographic conditions, showing a strong similarity to biofacies D (southern upwelling) and a decrease in the offshore biofacies A (Brazil Current front) and B (mixed oceanic and coastal waters). The percentages of *G. bulloides* and *G. calida* increased after 2.5 cal ka BP, and the percentage of *T. quinqueloba* increased after 2.0 cal ka BP (Fig. 7). These increases were associated with an increase in the percentage of *G. glutinata* and a decrease in the percentage of *G. ruber*, indicating a colder and more productive water column than in the previous phase. Thus, we can characterize this scenario as corresponding to a reduction of coastal inputs and strengthening and expansion of the upwelling system caused by stronger NE trade winds.

#### 5.5.2. Comparison of the *G. bulloides*/*G. ruber* (Gb/Gr) and cold/warm species (C/W) ratios

The cold events indicated by the *G. bulloides*/*G. ruber* (Gb/Gr) and cold/warm species (C/W) ratios coincided with the dominance of biofacies D between 4.0 and 3.5 cal kyr BP and after 2.5 cal ka BP. These correlations indicate that the intensity of upwelling increased these ratios, whereas the period between 9.0 and 6.0 cal kyr BP was dominated by biofacies C (northern upwelling) conditions, indicating lower-intensity cold events. The distinction between the two ratios during the cold period following 2.5 cal ka BP (Fig. 8) could be associated with the percentage of *T. quinqueloba* because this species occurred at low percentages prior to 2.0 cal ka BP (Fig. 7), and its percentages increased thereafter.

During the period between 6.0 and 2.5 cal kyr BP, the abundance ratios were similar (Fig. 8), indicating warm waters, but the biofacies and relative abundances (Figs. 7 and 9) did not suggest that this warming had been caused by the entry of Tropical Water into the CFUS. The maximum contribution of Tropical Water was recorded between 9.0 and 6.0 cal kyr BP, indicating an increase in biofacies A (Figs. 8 and 9). However, the occurrence of upwelling was marked by high percentages of *G. bulloides*, and the highest percentages of *G. bulloides* occurred at approximately 6.0 cal ka BP, in conjunction with *G. ruber*, thus maximizing the similarity with biofacies C.

After 6.0 cal ka BP, a decrease in the abundance of both *G. bulloides* and *G. ruber* was observed, with *G. bulloides* decreasing more dramatically, while increases in the abundances of *G. rubescens* and *G. glutinata* were recorded. These effects could indicate enhanced productivity levels and shelf water incursions and, thus, a rising influence of biofacies B. The decrease in the Gb/Gr ratio was associated with replacement of *G. bulloides* by *G. glutinata*, which indicated warm waters. These results suggest that the assertion that low Gb/Gr ratio values (tending to *G. ruber*) necessarily indicate oligotrophic conditions should be re-examined.

Alternatively, the warm period from 3.5–2.5 cal kyr BP could have been associated with more frequent Tropical Water incursions due to an increased similarity with oceanic biofacies compared with the upwelling biofacies, C and D (Fig. 9). Very low percentages of *G. bulloides* and *T. quinqueloba* and increases in *G. glutinata* and *G. ruber* were also observed (Fig. 7). These assemblage data indicate a substantial weakening of the CFUS and suggest that eddies may have been as important as or more important than the Cabo Frio upwelling for productivity. In this

case, the Gb/Gr ratio was better able to indicate warm waters than the C/W ratio but was not a better indicator of long-term oligotrophic conditions.

### 5.6. SST reconstructions via the MAT

Neither the SA nor SA + RJCM MAT model was able to reconstruct the SST variability in the CFUS, whereas the obtained minimum–maximum range (0.35 °C) was below the model error or RMSEP (Table 5). The lack of sensitivity can be explained by the interplay among different oceanographic features, such as the influence of the Brazil Current internal front, the presence of low salinity coastal water and the cold water from coastal upwelling, which represents shelf conditions. Such conditions may be responsible for the low spatial variation of the mean SST in the RJCM area (Fig. 2) as well as the lack of analog foraminifera assemblages compared with the applied database.

Although SST-MAT reconstructions have not been effective for estimating SST variability in the CFUS during the Holocene, the biofacies model showed significant variations (Fig. 9). This suggests that sub-surface layer may be the key to understanding climatic and oceanographic changes in the CFUS. SST variations are one of main factors controlling planktonic foraminifera assemblages, though other factors increase in importance at a local scale. According to Belem et al. (2013), the SACW (indicated by the 18 °C isotherm) is always present, varying from depths of 110 to 40 m between November 2010 and September 2011. Such phenomena in the photic zone could have favored the occurrence of two different types of conditions: the oligotrophic, clear surface layer, inhabited by warm-water species, and the cold, productive sub-surface layer, occupied by cold-water species. Then, variation in hydrodynamic processes in the sub-surface layer may have uncoupled the link between SST and the composition of the planktonic foraminifera assemblages. As the biofacies approach encompasses planktonic foraminifera living along the whole water column, surface and subsurface oceanographic features are already considered.

## 6. Conclusions

Analysis of planktonic foraminiferal assemblages in the RJCM using box-core tops yielded detailed information about the ecology of the structure of the planktonic foraminifera community within a 1° × 2.5° area in the Southwestern Atlantic. This analysis considered community differences in oceanic oligotrophic waters, oceanic productive waters, shelf waters and upwelling waters. This study also contributes to the understanding of the ecology of *G. rubescens*, which was found in shelf waters, and *G. calida*, which could be associated with upwelling-related productivity.

The RJCM planktonic foraminifera community was divided into four geographically and oceanographically distinct groups. This division favored the oceanographic biofacies definition, allowing its application in paleoceanography, using the similarity between recent assemblages (biofacies) and fossil assemblages. Biofacies A was related to the warm and oligotrophic waters of the Brazil Current; biofacies B was related to the mixture of oligotrophic (oceanic) and productive (shelf) waters, resulting in conditions of high temperature and productivity; biofacies C was related to the occurrence of upwelling events (cold and productive waters) attenuated by frequent Brazil Current intrusions (northern upwelling); and biofacies D was related to the occurrence of intense upwelling events (southern upwelling).

The application of the biofacies model to the fossil assemblages found in core CF10-01B indicated at least four major variations in the planktonic foraminifera community related to different oceanographic conditions over the last 9000 years in the CFUS. Such conditions may reflect atmospheric variations over the South Atlantic and the South American continent that influenced the variation of the upwelling and downwelling intensity by intensifying or weakening NE winds.

Comparison of the results of the SIMPER analysis and the analysis of the *G. bulloides*/*G. ruber* and cold/warm species abundance ratios showed that the abundance ratios were quite sensitive to upwelling events induced by NE winds. However, these analyses were more limited in relation to warm water because of the complexity of the CFUS, in which the source of nutrients is not restricted to the Cabo Frio upwelling, making it difficult to associate higher temperatures with lower productivity.

The addition of 34 box-core tops to the South Atlantic database improved the performance of the SST reconstructions generated through the MAT. However, the SST variation of 0.35 °C indicated during the Holocene was too small to reflect the real influence of upwelling on SSTs. Such small variations along the core could have been indicated either because the use of the MAT was not adequate or because the SST in the CFUS varied independently of the occurrence of upwelling. Other paleotemperature methods could be required to determine the cause of these small variations.

## Acknowledgments

This study was partially funded by the Conselho Nacional de Desenvolvimento Científico e Tecnológico (CNPq); CAPES, through a scholarship to DVL; and the “Institut de Recherche pour le Développement (IRD France)” – LMI PALEOTRACES. This study was also financially supported by the Geochemistry Network from PETROBRAS/CENPES and by the National Petroleum Agency (ANP) of Brazil (Grant 0050.004388.08.9). We thank Cristiano Chiessi (Universidade de São Paulo) for the Niebler and Gersonde (1998) South Atlantic database for the MAT analysis, and we thank the REVIZEE project for the foraminiferal box-core samples. A.L.S Albuquerque is a senior scholar from CNPq (National Council for the Development of Science and Technology, Brazil). Finally, we are especially grateful to the anonymous reviewers for their valuable comments, which strengthened the manuscript.

## Appendix A. Supplementary data

Supplementary data associated with this article can be found in the online version, at <http://dx.doi.org/10.1016/j.marmicro.2013.12.003>. These data include Google maps of the most important areas described in this article.

## References

- Absy, M.L., Cleef, A., Fournier, M., Martin, L., Servant, M., Sifeddine, A., da Silva, F.M., Soubies, F., Suguio, K., Turcq, B., Van der Hammen, T., 1991. Mise en évidence de quatre phases d'ouverture de la forêt dense dans le sud-est de l'Amazonie au cours des 60 000 dernières années. Première comparaison avec d'autres régions tropicales. *Comptes rendus de l'Académie des sciences. Série 2, Mécanique, Physique, Chimie, Sciences de l'univers, Sciences de la Terre*, 312(6), pp. 673–678.
- Albuquerque, A.L.S., Belem, A.L., Zuluaga, F.J.B., Cordeiro, L.G.M., Mendoza, U., Knoppers, B.A., Gurgel, M.H.C., Meyers, P.A., Capilla, R., 2014. Particulate fluxes and bulk geochemical characterization of the Cabo Frio Upwelling System in Southeastern Brazil: sediment trap experiments between spring 2010 and summer. *An. Acad. Bras. Cienc.* 84 (2) (in press).
- Al-Sabouni, N., Kucera, M., Schmidt, D.N., 2007. Vertical niche separation control of diversity and size disparity in planktonic foraminifera. *Mar. Micropaleontol.* 63 (1–2), 75–90.
- Anand, P., Elderfield, H., Conte, M.H., 2003. Calibration of Mg/Ca thermometry in planktonic foraminifera from a sediment trap time series. *Paleoceanography* 18 (2), 1–15 (28).
- Angulo, R.J., Lessa, G.C., 1997. The Brazilian sea-level curves: a critical review with emphasis on the curves from the Paranaguá and Cananéia regions. *Mar. Geol.* 140 (1), 141–166.
- Angulo, R.J., Souza, M.C.D., Reimer, P., Sasaoca, S.K., 2005. Reservoir effect of the southern and southeastern Brazilian coast. *Radiocarbon* 47 (1–7).
- Bard, E., 1998. Geochemical and geophysical implications of the radiocarbon calibration. *Geochimica et Cosmochimica Acta*. 62 (12), 2025–2038.
- Bé, A.W.H., 1977. An ecological, zoogeographic and taxonomic review of recent planktonic foraminifera. In: Ramsay, A.T.S. (Ed.), *Oceanic Micropalaeontology*. Academic Press, London, pp. 1–100.
- Bé, A.W.H., Hamlin, W.H., 1967. Ecology of recent planktonic foraminifera: part 3: distribution in the North Atlantic during the summer of 1962. *Micropalaeontology* 13 (1), 87–106.
- Bé, A.W.H., Tolderlund, D.S., 1971. Distribution and ecology of living planktonic foraminifera in surface waters of the Atlantic and Indian Oceans. In: Funnell, B.M., Riedel, W.R.

- (Eds.), *The Micropaleontology of the Oceans*. Cambridge University Press, New York, pp. 105–139.
- Belem, A.L., Castelão, R.M., Albuquerque, A.L.S., 2013. Controls of subsurface temperature variability in a western boundary upwelling system. *Geophys. Res. Lett.* 40, 1–5.
- Bijma, J., Faber, W.W., Hemleben, C., 1990. Temperature and salinity limits for growth and survival of some planktonic foraminifera in laboratory cultures. *J. Foraminif. Res.* 20 (2), 95–116.
- Blaauw, M., 2010. Methods and code for 'classical' age-modeling of radiocarbon sequences. *Quat. Geochronol.* 5, 512–518.
- Boltovskoy, E., 1962. Planktonic foraminifera as indicators of different water masses in the South Atlantic. *Micropaleontology* 8 (3), 403–408.
- Boltovskoy, E., Boltovskoy, D., Correa, N., Brandini, F., 1996. Planktonic foraminifera from the southwestern Atlantic (30°–60°S): species-specific patterns in the upper 50 m. *Mar. Micropaleontol.* 28 (1), 53–72.
- Calado, L., Gangopadhyay, A., da Silveira, I.C.A., 2006. A parametric model for the Brazil Current meanders and eddies off southeastern Brazil. *Geophys. Res. Lett.* 33, L12602.
- Calado, L., Silveira, I.C.A., Gangopadhyay, A., de Castro, B.M., 2010. Eddy-induced upwelling off Cape São Tomé (22°S, Brazil). *Cont. Shelf Res.* 30 (10–11), 1181–1188.
- Campos, E.J.D., Velhote, D., Silveira, I.C.A., 2000. Shelf break upwelling driven by Brazil Current cyclonic meanders. *Geophys. Res. Lett.* 27, 751–754.
- Caron, D.A., Bé, A.W., Anderson, O.R., 1981. Effects of variations in light intensity on life processes of the planktonic foraminifer *Globigerinoides sacculifer* in laboratory culture. *J. Mar. Biol. Assoc. U. K.* 62 (2), 435–451.
- Carvalho, L.M.V., Carvalho, L.M.V., Jones, C., Liebmann, B., 2004. The South Atlantic Convergence Zone: intensity, form, persistence and relationships with intraseasonal to interannual activity and extreme rainfall. *J. Clim.* 17 (1), 88–108.
- Chiessi, C.M., Ulrich, S., Multiza, S., Pätzold, J., Wefer, G., 2007. Signature of the Brazil–Malvinas Confluence (Argentine Basin) in the isotopic composition of planktonic foraminifera from surface sediments. *Mar. Micropaleontol.* 64 (1–2), 52–66.
- Clarke, K.R., 1993. Non-parametric multivariate analyses of changes in community structure. *Aust. J. Ecol.* 18, 117–143.
- Coloma, C., Marchant, M., Hebbeln, D., 2005. Planktonic foraminifera during El Niño 1997–98 off Coquimbo (30°S; 73°W), Chile. *Gayana* 69 (1), 48–77.
- Corrêa, I.C.S., 1996. Les variations du niveau de la mer durant les derniers 17500 ans BP: l'exemple de la plate-forme continentale du Rio Grande do Sul. *Brésil. Marine Geology*. 130, 163–178.
- Cruz, F.W., Vuille, M., Burns, S.J., Wang, X., Cheng, H., Werner, M., Edwards, R.L., Karmann, I., Auler, A.S., Nguyen, H., 2009. Orbitally driven east–west antiphasing of South American precipitation. *Nat. Geosci.* 2, 210–214.
- Ding, X., Bassinot, F., Guichard, F., Li, Q.Y., Fang, N.Q., Labeyrie, L., Xin, R.C., Adisaputra, M.K., Hardjajidjaksana, K., 2006. Distribution and ecology of planktonic foraminifera from the seas around the Indonesian Archipelago. *Mar. Micropaleontol.* 58 (2), 114–134.
- Eguchi, N.O., Kawahata, H., Taira, A., 1999. Seasonal response of planktonic foraminifera to surface ocean condition: sediment trap results from the Central North Pacific Ocean. *J. Oceanogr.* 55, 681–691.
- Haug, G.H., Hughen, K.A., Sigman, D.M., Peterson, L.C., Röhl, U., 2001. Southward migration of the Intertropical Convergence Zone through the Holocene. *Science* 293 (5533), 1304–1308.
- Hilbrecht, H., 1997. Morphologic gradation and ecology in *Neoglobobulimina pachyderma* and *N. dutertrei* (planktonic foraminifera) from core top sediments. *Mar. Micropaleontol.* 31 (1), 31–43.
- Hutson, N.H., 1980. The Agulhas current during the late Pleistocene: analysis of modern faunal analogs. *Science* 207, 64–66.
- Kennett, J.P., Srinivasam, M.S., 1983. *Neogene Planktonic Foraminifera: A Phylogenetic Atlas*. Hutchinson Ross Publishing Company, Stroudsburg (273 pp.).
- Kruskal, J.B., 1964. Multidimensional scaling by optimizing goodness of fit to a nonmetric hypothesis. *Psychometrika* 29, 1–27.
- Kucera, M., 2007. Planktonic foraminifera as tracer of past oceanic environments. In: *Hillaire-Marcel, C., Vernal, A.D. (Eds.), Proxies in Late Cenozoic Paleooceanography*. Elsevier, Tokyo (213–255 pp.).
- Kucera, M., Weinelt, M., Kiefer, T., Pflaumann, U., Hayes, A., Weinelt, M., Chen, M., Mix, A.C., Barrows, T.T., Cortijo, E., Duprat, J., Juggins, S., Waelbroeck, C., 2005. Reconstruction of sea-surface temperatures from assemblages of planktonic foraminifera: multi-technique approach based on geographically constrained calibration data sets and its application to glacial Atlantic and Pacific Oceans. *Quat. Sci. Rev.* 24 (7), 951–998.
- Kuroyanagi, A., Kawahata, H., 2004. Vertical distribution of living planktonic foraminifera in the seas around Japan. *Mar. Micropaleontol.* 53 (1–2), 173–196.
- Laslandes, S., Sylvestre, F., Sifeddine, A., Turcq, B., Albuquerque, A.L.S., Abrão, J., 2005. Enregistrement de la variabilité hydroclimatique au cours des 6500 dernières années sur le littoral de Cabo Frio (Rio de Janeiro, Brésil). *Compt. Rendus Geosci.* 338, 667–675.
- Lidz, L., 1966. Deep-sea Pleistocene biostratigraphy. *Science* 154, 1448–1452.
- Little, M.G., Schneider, R.R., Kroon, D., Price, B., Bickert, T., Wefer, G., 1997. Rapid paleoceanographic changes in the Benguela Upwelling System for the last 160,000 years as indicated by abundances of planktonic foraminifera. *Palaeogeogr. Palaeoclimatol. Palaeoecol.* 130 (1–4), 135–161.
- Loeblich, A.R., Tappan, H., 1988. *Foraminiferal Genera and Their Classification*. Van Nostrand Reinhold, New York (211 pp.).
- Machain-Castillo, M.L., Monreal-Gómez, M.A., Arellano-Torres, E., Merino-Ibarra, M., González-Chávez, G., 2008. Recent planktonic foraminiferal distribution patterns and their relation to hydrographic conditions of the Gulf of Tehuantepec, Mexican Pacific. *Mar. Micropaleontol.* 66 (2), 103–119.
- Malmgren, B.A., Kucera, M., Nyberg, J., Waelbroeck, C., 2001. Comparison of statistical and artificial neural network techniques for estimating past sea surface temperatures from planktonic foraminiferal census data. *Paleoceanography* 16, 1–11.
- Martinez, J.L., Taylor, L., De Deckker, P., Barrows, T., 1998. Planktonic foraminifera from the eastern Indian Ocean: distribution and ecology in relation to the Western Pacific Warm Pool (WPWP). *Mar. Micropaleontol.* 34 (3), 121–151.
- Martinez, J.L., Mora, G., Barrows, T.T., 2007. Paleooceanographic conditions in the western Caribbean Sea for the last 560 cal kyr BP as inferred from planktonic foraminifera. *Mar. Micropaleontol.* 64 (3–4), 177–188.
- Multiza, S., Boltovskoy, D., Donner, B., Meggers, H., Paul, A., Wefer, G., 2003. Temperature:  $\delta^{18}\text{O}$  relationships of planktonic foraminifera collected from surface waters. *Palaeogeogr. Palaeoclimatol. Palaeoecol.* 202, 143–152.
- Naidu, P.D., 2007. Influence of monsoon upwelling on the planktonic foraminifera off Oman during Late Quaternary. *Indian J. Mar. Syst.* 36 (4), 322–331.
- Niebler, H.S., Gersonde, R., 1998. A planktonic foraminiferal transfer function for the southern South Atlantic Ocean. *Mar. Micropaleontol.* 34 (3–4), 213–234.
- Niebler, H.S., Hubberten, H.W., Gersonde, R., 1999. Oxygen isotope values of planktonic foraminifera: a tool for the reconstruction of surface water stratification. In: *Fischer, G., Wefer, G. (Eds.), Use of Proxies in Palaeoceanography*. Springer-Verlag, Berlin Heidelberg, pp. 165–189.
- Peeters, F.J.C., Acheson, R., Brummer, G.J.A., de Ruijter, W.P.M., Schneider, R.R., Ganssen, G.M., Ufkes, E., Kroon, D., 2004. Vigorous exchange between the Indian and Atlantic oceans at the end of the past five glacial periods. *Nature* 430, 661–665.
- Pflaumann, U., Duprat, J., Pujol, C., Labeyrie, L.D., 1996. SIMMAX: a modern analog technique to deduce Atlantic sea surface temperatures from planktonic foraminifera in deep-sea sediments. *Paleoceanography* 11 (1), 15–35.
- Pivel, M.A.G., Santarosa, A.C.A., Toledo, F.A.L., Costa, K.B.C., 2013. The Holocene onset in the southwestern South Atlantic. *Palaeogeogr. Palaeoclimatol. Palaeoecol.* 374, 164–172.
- Portilho-Ramos, R.C., Rios-Neto, A.M., Barbosa, C.F., 2006. Caracterização bioestratigráfica do Neógeno superior da Bacia de Santos com base em foraminíferos planctônicos. *Rev. Bras. Paleontol.* 9 (3), 349–354.
- Prado, L.F., Wainer, I., Chiessi, C.M., Ledru, M.P., Turcq, B., 2012. Mid-Holocene climate reconstruction for eastern South America. *Clim. Past Discuss.* 8, 5925–5961.
- Rasmussen, T.L., Thomsen, E., 2011. Changes in planktonic foraminiferal faunas, temperature and salinity in the Gulf Stream during the last 30,000 years: influence of meltwater via the Mississippi River. *Quat. Sci. Rev.* 33, 42–54.
- Ravelo, A.C., Fairbanks, R.G., Philander, S.G.H., 1990. Reconstructing tropical Atlantic hydrography using planktonic foraminifera and an ocean model. *Paleoceanography* 5 (3), 409–431.
- Razik, S., Chiessi, C.M., Romero, O.E., von Dobeneck, T., 2013. Interaction of the South American Monsoon System and the Southern Westerly Wind Belt during the last 14 kyr. *Palaeogeogr. Palaeoclimatol. Palaeoecol.* 374, 28–40.
- Reimer, P.J., Baillie, M.G.L., Bard, E., Bayliss, A., Beck, J.W.B., Paul, G., Ramsey, C., Bronk, B., Cailin, E., Burr, G.S., Edwards, R.L., Friedrich, M., Grootes, P.M., Guilderson, T.P., Hajdas, I., Heaton, T.J., Hogg, A.G., Hughen, K.A., Kaiser, K.F., Kromer, B., McCormac, F.G., Manning, S.W., Reimer, R.W., Richards, D.A., Southon, J.R., Talamo, S., Turney, C.S.M., Van Der Plicht, J., Weyhenmeyer, C.E., 2009. Intcal09 and Marine09 radiocarbon age calibration curves, 0–50,000 years cal BP. *Radiocarbon* 51 (4), 1111–1150.
- Rossi-Wongtschowski, C.L.B., Madureira, L.S.P., 2006. O Ambiente oceanográfico da plataforma continental e do talude na região sudeste-sul do Brasil. *EdUSP, São Paulo* (466 pp.).
- Schmuker, B., Schiebel, R., 2002. Planktonic foraminifera and hydrography of the eastern and northern Caribbean Sea. *Mar. Micropaleontol.* 46 (3–4), 387–403.
- Sifeddine, A., Martin, L., Turcq, B., Volkmer-Ribeiro, C., Soubiès, F., Cordeiro, R.C., Suguio, K., 2001. Variations of the Amazonian rainforest environment: a sedimentological record covering 30,000 years. *Palaeogeogr. Palaeoclimatol. Palaeoecol.* 168 (3), 221–235.
- Silveira, I.C.A., Schmidt, A.C.K., Campos, E.J.D., Godoi, S.S., Ikeda, Y., 2000. A Corrente do Brasil ao largo da costa leste brasileira. *Rev. Bras. Oceanogr.* 48 (2), 171–183.
- Souto, D.D., Lessa, D.V.O., Albuquerque, A.L.S., Sifeddine, A., Turcq, B.J., Barbosa, C.F., 2011. Marine sediments from southeastern Brazilian continental shelf: a 1200 year record of upwelling productivity. *Palaeogeogr. Palaeoclimatol. Palaeoecol.* 299 (1–2), 49–55.
- Stemann, T.A., Johnson, K.G., 1992. Coral assemblages, biofacies, and ecological zones in the mid-Holocene reef deposits of the Enriquillo Valley, Dominican Republic. *Lethaia* 25 (3), 231–241.
- Stramma, L., England, M., 1999. On the water masses and mean circulation of the South Atlantic Ocean. *Journal of Geophysical Research*. 104 (C9), 20,863–20,883.
- Thunell, R.C., 1978. Distribution of recent planktonic foraminifera in surface sediments of the Mediterranean Sea. *Mar. Micropaleontol.* 3 (2), 147–173.
- Tolderlund, D.S., Bé, A.W.H., 1971. Seasonal distribution of planktonic foraminifera in the Western North Atlantic. *Micropaleontology* 17 (3), 297–329.
- Toledo, F.A.L., Costa, K.B., Pivel, M.A.G., Campos, E.J.D., 2008. Tracing past circulation changes in the Western South Atlantic based on planktonic foraminifera. *Rev. Bras. Paleontol.* 11 (3), 169–178.
- Turcq, B., Albuquerque, A.L.S., Cordeiro, R.C., Sifeddine, A., Simoes Filho, F.F.L., Souza, A.G., Abrão, J.J., Oliveira, F.B.L., Silva, A.O., Capitão, J., 2002. Accumulation of organic carbon in five Brazilian lakes during the Holocene. *Sediment. Geol.* 148 (1–2), 319–342.
- Valentin, J.L., 1984. Analyse des paramètres hydrobiologiques dans la remontée de Cabo Frio (Brésil). *Mar. Biol.* 82 (3), 259–276.
- Vicalvi, M.A., 1997. Zonamento bioestratigráfico e paleoclimático dos sedimentos do Quaternário superior do talude da Bacia de Campos, RJ, Brasil. *Bol. Geociências Petrobras* 11 (1/2), 132–165 (Rio de Janeiro).
- Waelbroeck, C., Labeyrie, L., Duplessy, J.-C., Guiof, J., Labracherie, M., Leclaire, H., Duprat, J., 1998. Improving past sea surface temperature estimates based on planktonic fossil faunas. *Paleoceanography* 13 (3), 272–283.